Seismic Multi-Axial Behavior of Concrete-Filled Steel Tube Beam-Columns

Mark Denavit

Jerome F. Hajjar

University of Illinois at Urbana-Champaign
Urbana, Illinois

Tiziano Perea

Roberto T. Leon

Georgia Institute of Technology
Atlanta, Georgia

Sponsors: National Science Foundation
American Institute of Steel Construction
Georgia Institute of Technology
University of Illinois at Urbana-Champaign

August 14, 2009

Introduction

- NEESR-II: System Behavior Factors for Composite and Mixed Structural Systems
- Analytical Investigation
  - Following prior work focusing on RCFT members and extending to CCFT and SRC members
  - Three-dimensional distributed plasticity mixed beam element formulation
  - Comprehensive uniaxial cyclic constitutive models for concrete core and steel tube
  - Parametric Studies
    - Developing rational system response factors (ATC-63)
    - Investigations of beam-column strength
    - Establishing guidelines for the computation of equivalent composite beam-column rigidity to be used in seismic analysis and design of composite frames
- Experimental Investigation

Element Formulation

- Three-dimensional distributed plasticity mixed beam element formulation
- Mixed basis allows for accurate analysis of material and geometric nonlinearity
  - Interpolation functions for both element displacements and forces
- Formulated in the corotational frame
- Implemented within the OpenSees framework
  - Suitable for static and dynamic analyses
  - Utilizes built in coordinate transformations and sections

Concrete Backbone Curve

Increasing post-peak degradation with increasing *f′c*

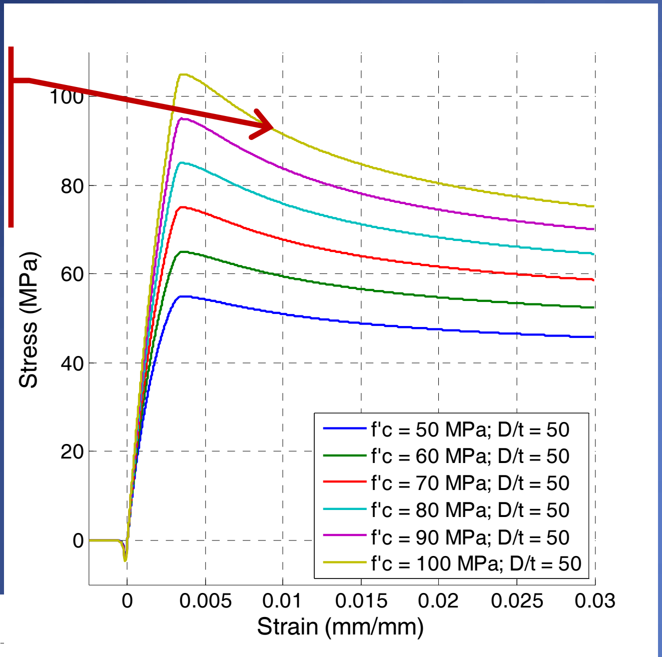

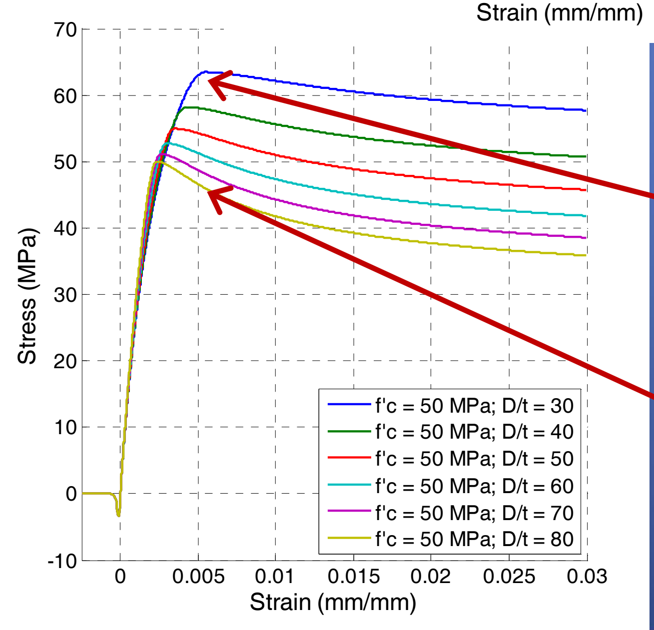

Increasing strength with decreasing *D/t*

Increasing post-peak degradation with increasing *D/t*

Backbone curve in tension and compression based on the model by Tsai (1988)

Compression:

- Initial stiffness: $E_c\left[\mathrm{MPa}\right]=8,200\, f_c'\left[\mathrm{MPa}\right]^{3/8}$
- Peak stress: $f_{cc}' = f_c'\left(-1.254+2.254\sqrt{1+\frac{7.94 f_l}{f_c'}}-2\frac{f_l}{f_c'}\right)$
  - Confinement Pressure: $f_l=\alpha_\theta F_y \frac{2}{D/t-2}$
  - Hoop Stress Ratio: $\alpha_\theta = 0.138-0.00174\left(D/t\right)\geq 0$
- Strain at peak stress: $\varepsilon_{cc}'=\varepsilon_c\left(1+5\left(f_{cc}'/f_c'-1\right)\right)$
- Post peak factor *r*:

$$r^{-}=\begin{cases} f_c'\left[\mathrm{MPa}\right]/5.2-1.9 & \text{for } \varepsilon>\varepsilon_{cc}' \\ 0.4+0.016\left(D/t\right)\left(f_c'/F_y\right) & \text{for } \varepsilon\leq\varepsilon_{cc}' \end{cases}$$

Steel Backbone Curve

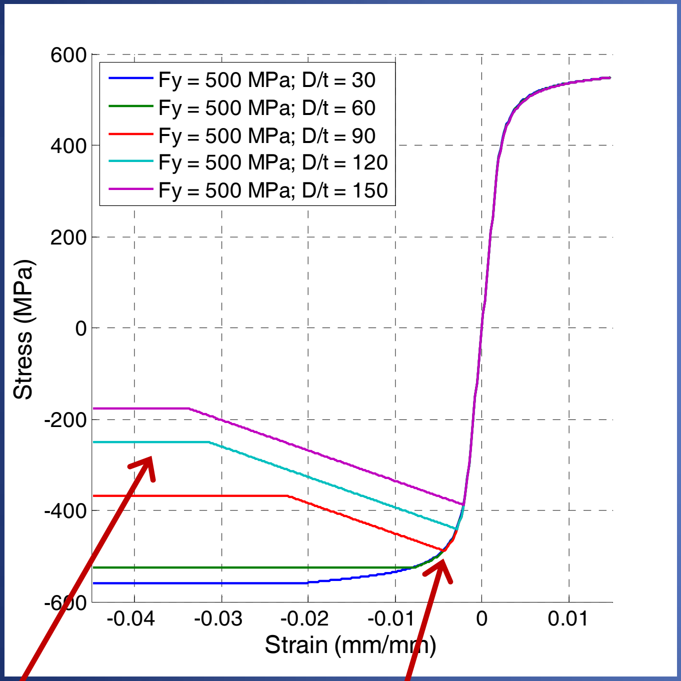

Decreasing residual stress with increasing *D/t*

Decreasing local buckling strain with increasing *D/t*

Plasticity model based on the incremental bounding surface formulation by Shen et al. (1995) with modifications for CCFT members

Local Buckling:

$$R = \frac{D}{t}\frac{F_y}{E_s}$$

- Strain at initial local buckling: $\varepsilon_{lb} = \varepsilon_y \left(0.2139 R^{-1.413}\right)$
- Residual stress: $f_{rs} = \begin{cases} f_{lb}\left(R_{crit}/R\right) & \text{for } R > R_{crit} = 0.17 \\ f_{lb} & \text{otherwise} \end{cases}$
- Degradation slope: $K_s = -\frac{E_s}{30}$

Residual Stresses:

- Initial plastic Strain: 0.0006

CCFT Model Validation

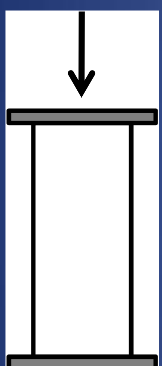

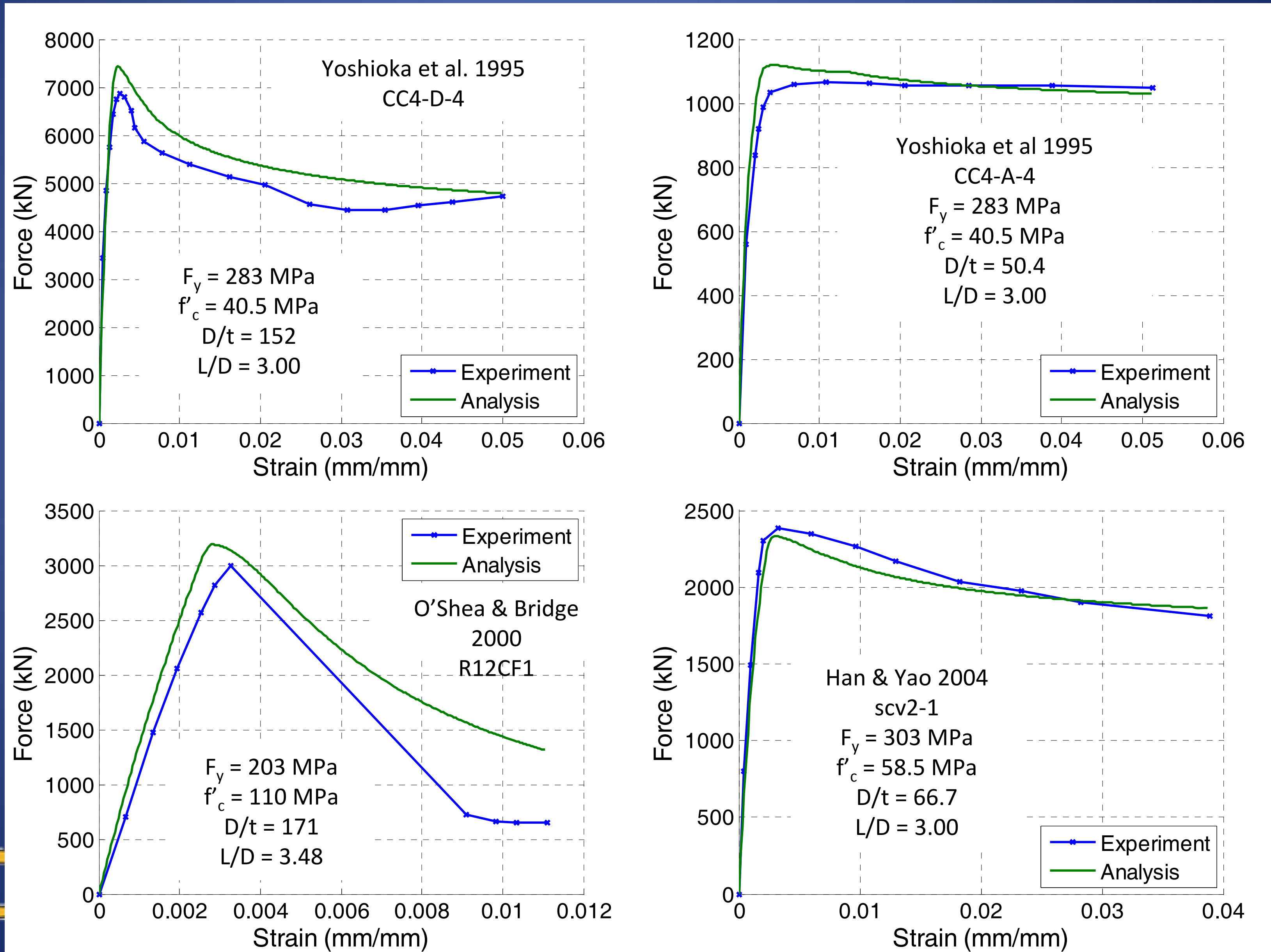

CCFT Model Validation

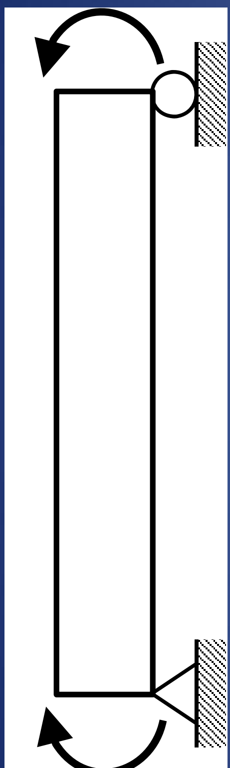

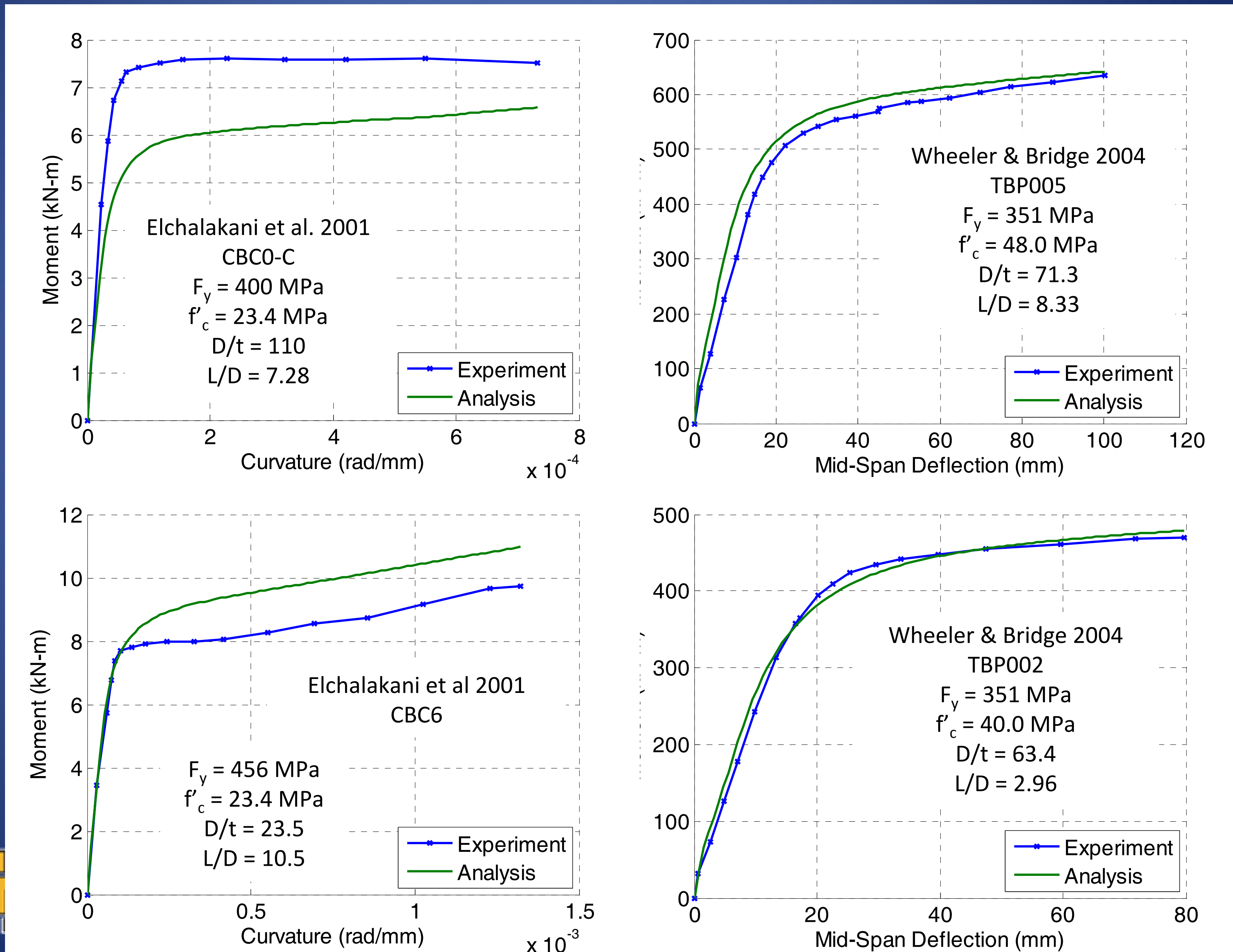

CCFT Model Validation

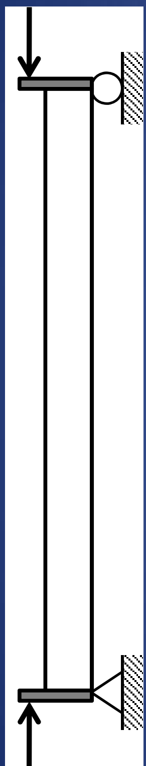

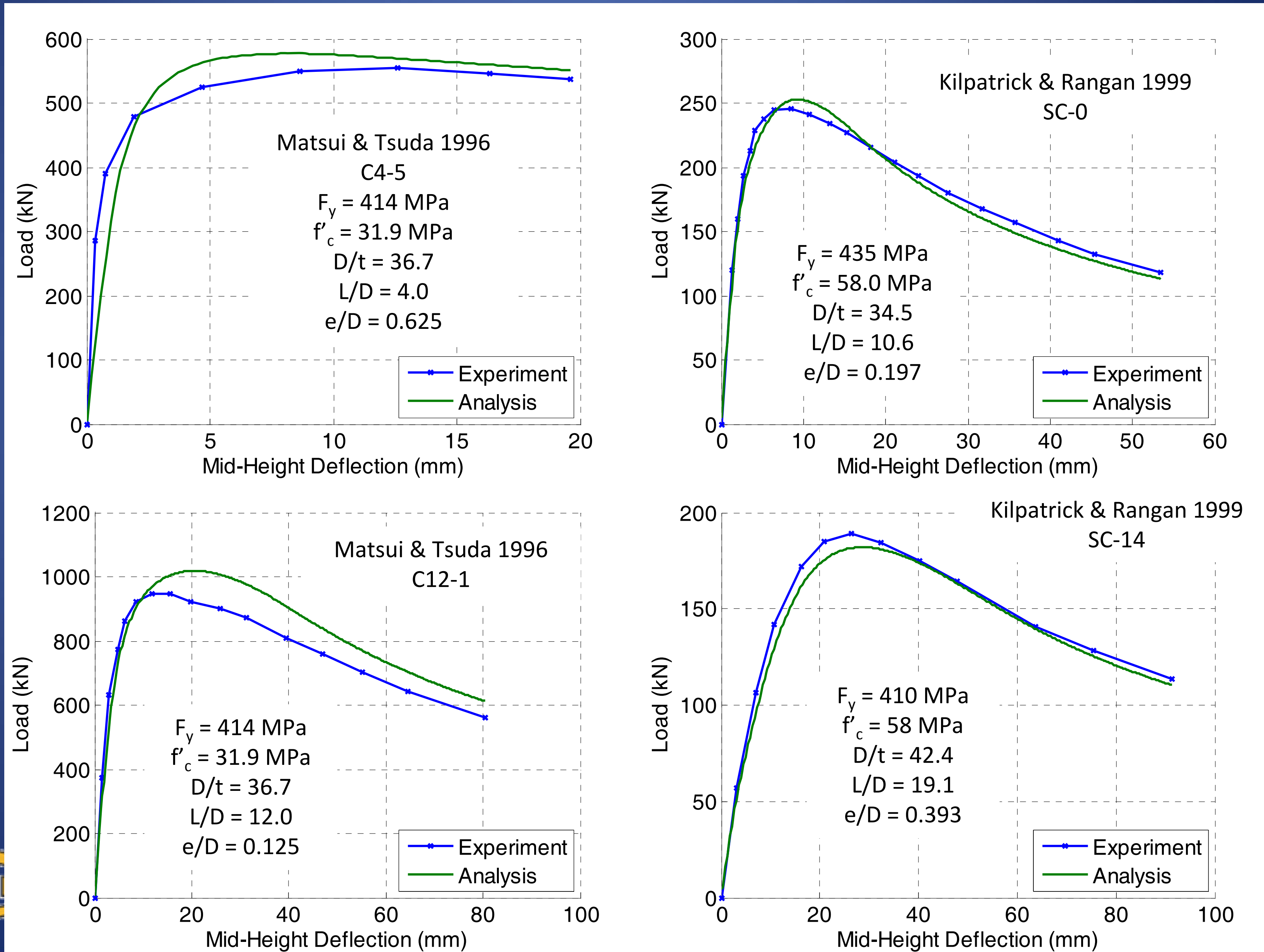

CCFT Model Validation

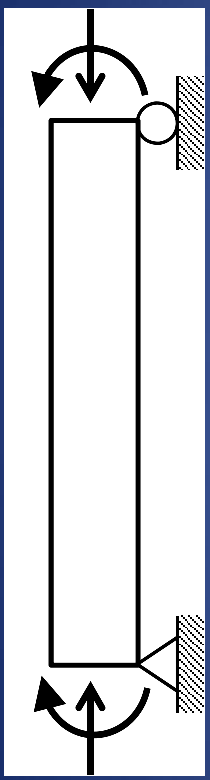

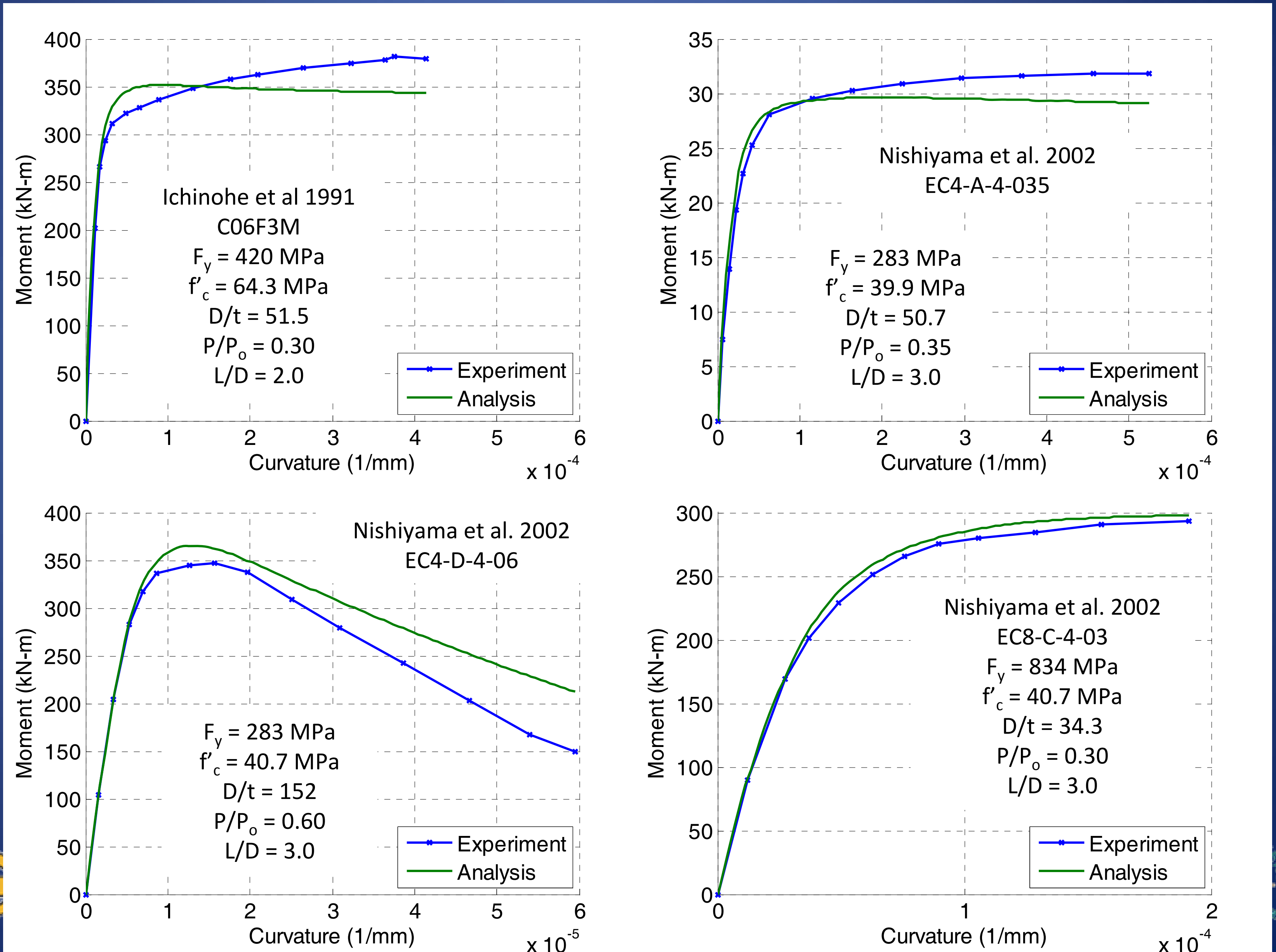

Cyclic Behavior

Steel

Cyclic plasticity model by Shen et al. (1995)

- Elastic unloading
- Decreasing elastic zone
- Bauschinger effect
- Bounding stiffness

Local buckling degradation

- Elastic range: $\kappa_{reduced} = \gamma_\kappa \kappa$

$$\gamma_k = \left(1 - 15R\sqrt{\frac{W^p}{F_y}}\right) \geq 0.05$$

- Plastic modulus: $E^p_{reduced} = \gamma_{E^p} E^p$

$$\gamma_{E^p} = \left(1 - 10R\sqrt{\frac{W^p}{F_y}}\right) \geq 0.05$$

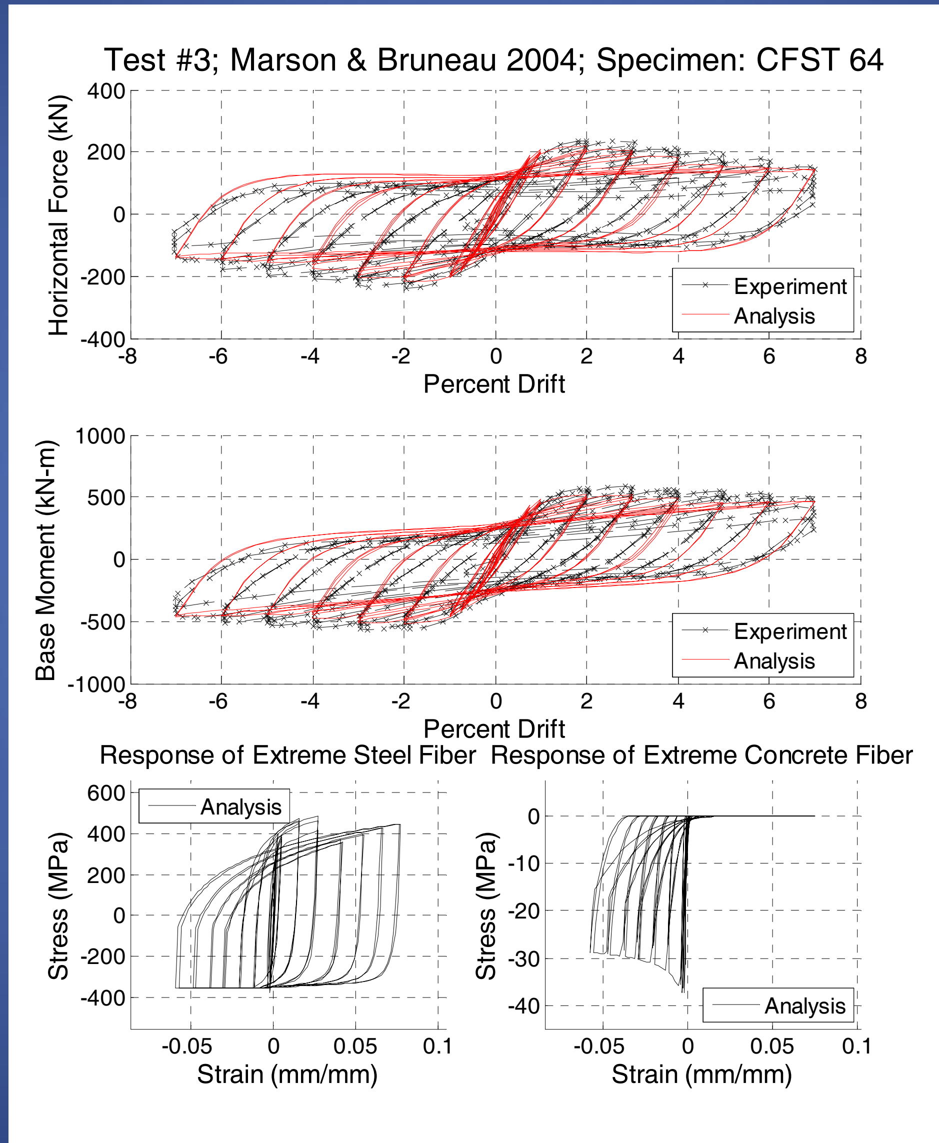

D = 406 mm; *t* = 5.50 mm; f'_c = 37 MPa; F_y = 449 MPa;
L = 2,200 mm; *P* = 1,000 kN

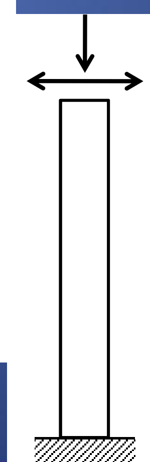

Concrete

Rule based model by Chang and Mander (1994)

Smooth nonlinear unloading, reloading, and transition curves

- Cyclic tension
- Opening and closing of cracks

Cyclic Model Validation

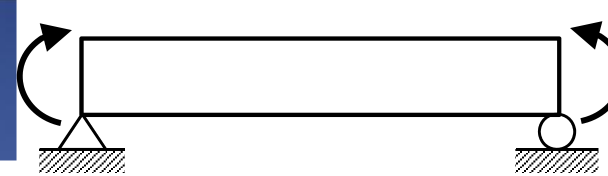

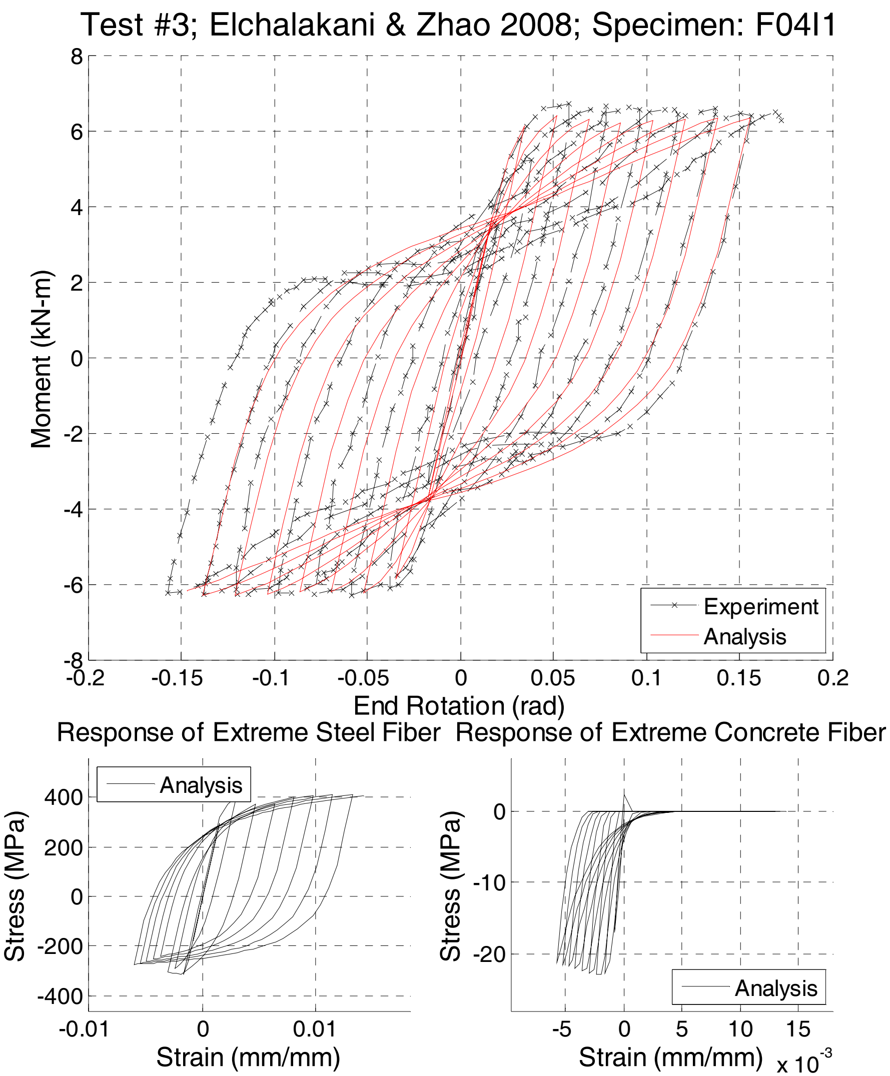

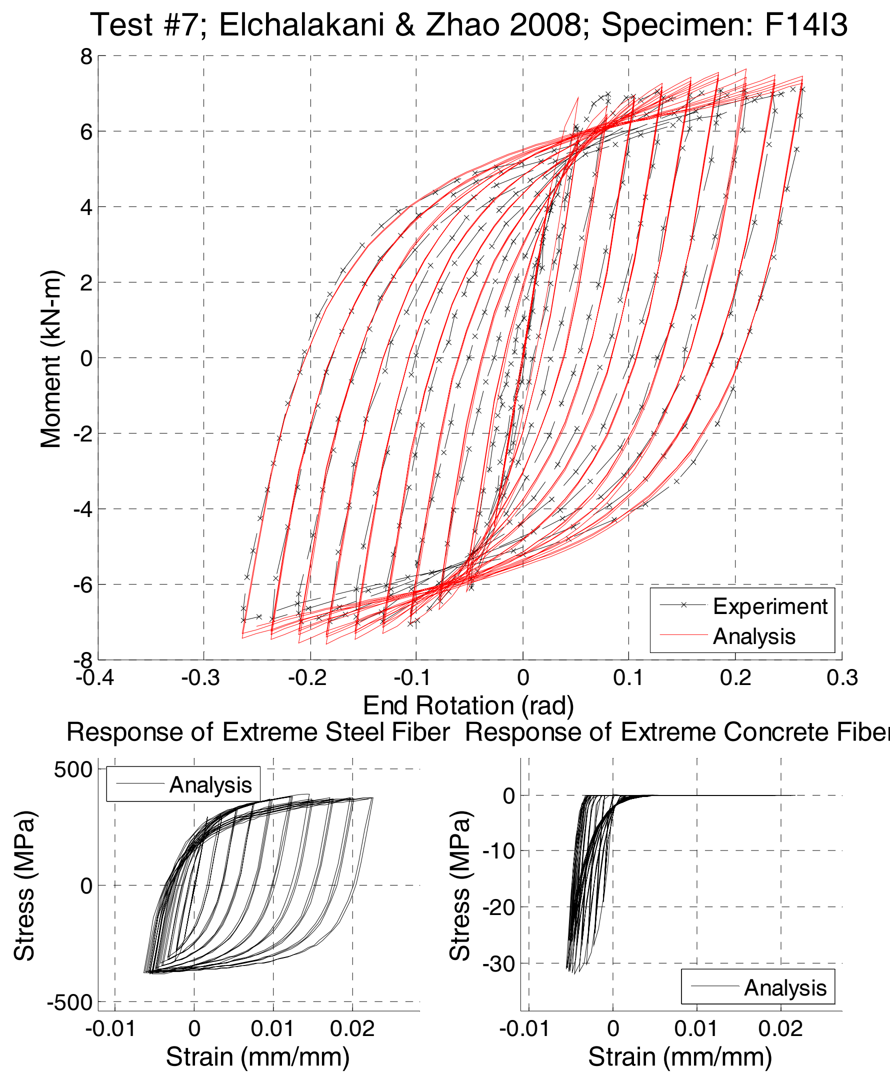

D = 110 mm; t = 1.25 mm; f'_c = 23.1 MPa; F_y = 430 MPa
L = 800 mm

D = 89.3 mm; t = 2.52 mm; f'_c = 23.1 MPa; F_y = 378 MPa
L = 800 mm

Full-Scale Beam-Column Tests

- Specimens chosen to fill gaps in prior experimental research, namely high member slenderness and section slenderness
- Experimentally determine
  - Progression of bending stiffness ($EI_{effective}$)
  - Beam-column interaction strength, including stability effects
  - Post-peak behavior and progression of damage of members subjected to large cyclic deformations
- Provide complex set of data for validation of computational models

MAST Facility

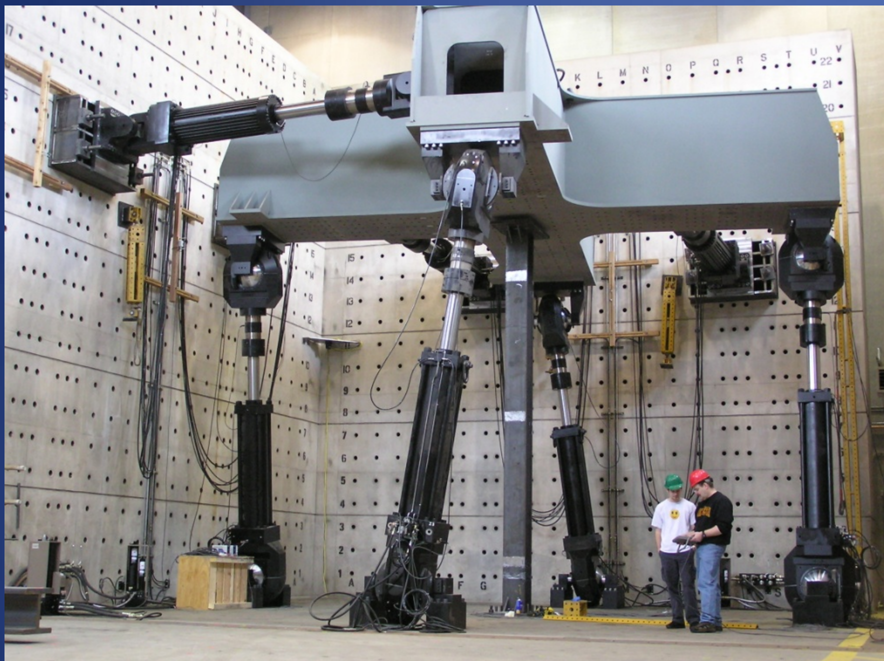

NEES@Minnesota

The MAST facility permits the comprehensive testing of a wide range of composite beam-columns subjected to three dimensional loading at a realistic scale.

Maximum non-concurrent capacities of MAST DOFs

Degree of Freedom	Load	Stroke/ Rotation
X-Translation	±3,910 kN	±406 mm
X-Rotation	±12,080 kN-m	±7°
Y-Translation	±3910 kN	±406 mm
Y-Rotation	±12,080 kN-m	±7°
Z-Translation	±5,870 kN	±508 mm
Z-Rotation	±17,900 kN-m	±10°

Measured Properties

Specimen	HSS steel L (mm) measured	t (mm) measured	F_y (MPa) coupon	F_u (MPa) coupon	E_s (MPa) coupon	Concrete f'$_c$ (MPa) measured	E_c (MPa) measured	f_t (MPa) measured
1-CCFT5.563x0.134-18ft-5ksi	5,499	3.24	383.4	487.6	193,984	37.92	27,579	7.58
2-CCFT12.75x0.25-18ft-5ksi	5,499	5.80	337.1	446.2	199,162	37.92	27,579	7.58
3-CCFT20x0.25-18ft-5ksi	5,525	5.98	328.0	470.7	200,262	37.92	27,579	7.58
4-RCFTw20x12x0.3125-18ft-5ksi	5,537	7.15	365.4	501.7	202,375	37.92	27,579	7.58
5-RCFTs20x12x0.3125-18ft-5ksi	5,537	7.15	365.4	501.7	202,375	37.92	27,579	7.58
6-CCFT12.75x0.25-18ft-12ksi	5,499	5.80	337.1	446.2	199,162	87.56	41,851	11.38
7-CCFT20x0.25-18ft-12ksi	5,534	5.98	328.0	470.7	200,262	87.56	41,851	11.38
8-RCFTw20x12x0.3125-18ft-12ksi	5,553	7.15	365.4	501.7	202,375	87.56	41,851	11.38
9-RCFTs20x12x0.3125-18ft-12ksi	5,553	7.15	365.4	501.7	202,375	87.56	41,851	11.38
10-CCFT12.75x0.25-26ft-5ksi	7,950	5.80				50.33	35,094	3.79
11-CCFT20x0.25-26ft-5ksi	7,995	5.98	328.0	470.7	200,262	50.33	35,094	3.79
12-RCFTw20x12x0.3125-26ft-5ksi	7,957	7.15	365.4	501.7	202,375	50.33	35,094	3.79
13-RCFTs20x12x0.3125-26ft-5ksi	7,969	7.15	365.4	501.7	202,375	50.33	35,094	3.79
14-CCFT12.75x0.25-26ft-12ksi	7,950	5.80				79.29	37,921	11.03
15-CCFT20x0.25-26ft-12ksi	7,976	5.98				79.29	37,921	11.03
16-RCFTw20x12x0.3125-26ft-12ksi	7,976	7.15				79.29	37,921	11.03
17-RCFTs20x12x0.3125-26ft-12ksi	7,976	7.15				79.29	37,921	11.03
18-CCFT5.563x0.134-26ft-12ksi	7,976	3.24	383.4	487.6	193,984	79.29	37,921	11.03

Setup and Instrumentation

- Strain Gages
  - Uniaxial and Rosettes Distributed Along Height
  - Measurements during concrete pouring and testing
- LVDTs
  - Sets of three for biaxial curvature measurement
- String Pots
  - Distributed along height
- Krypton Coordinate Measurement Machine
- Video and Still Images
  - Four towers for images of whole specimen as well as base

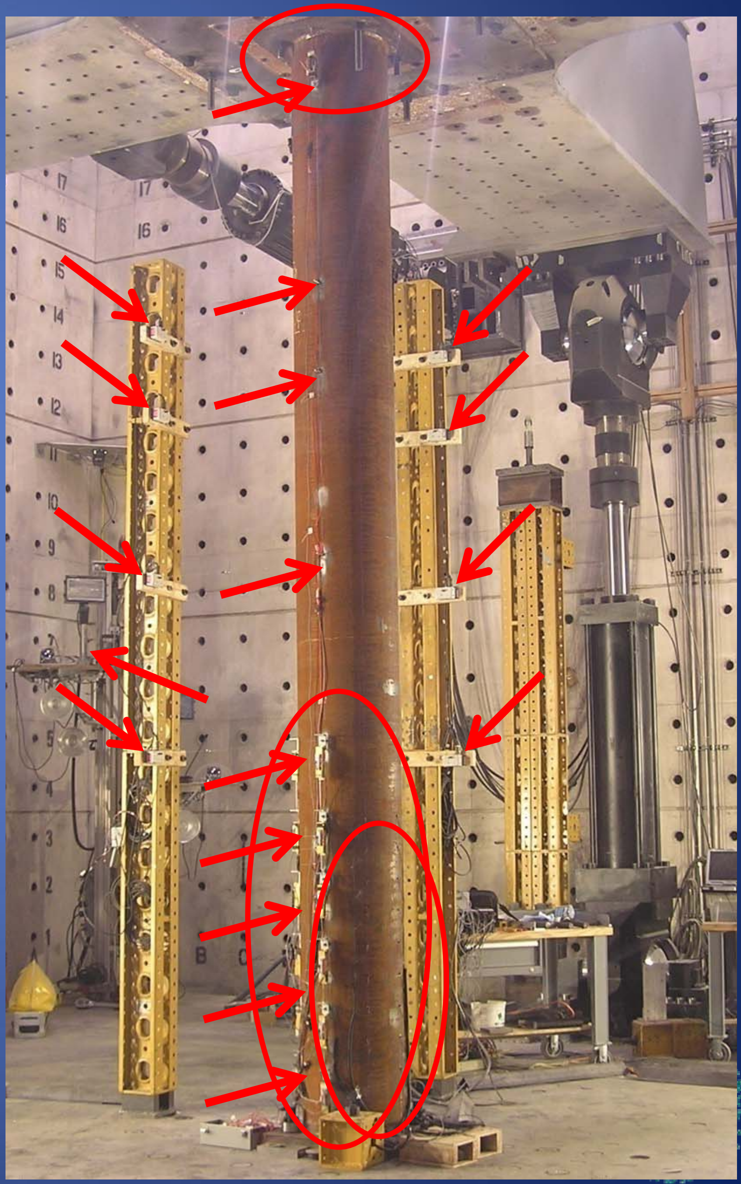

Typical Load Protocol

Load Case 1:
Concentric Loading

Load Case 2-3:
Uniaxial Cyclic

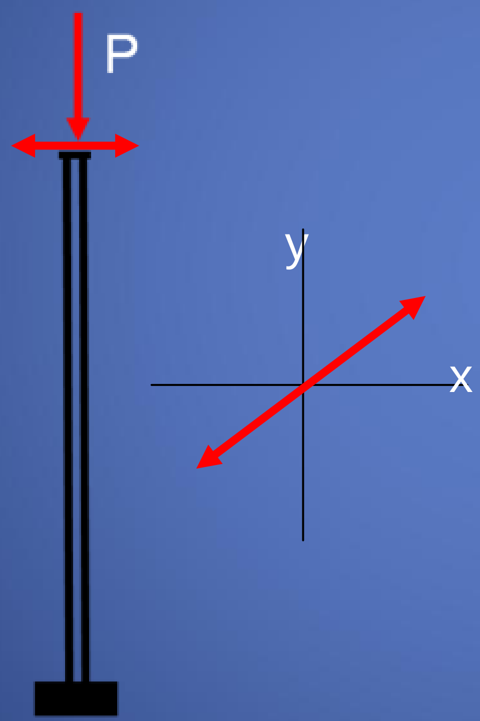

Load Case 4-6:
Biaxial Cyclic

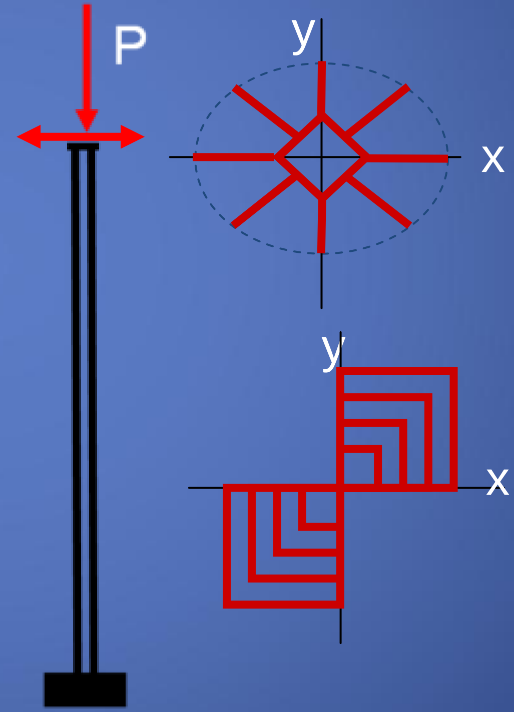

Load Case 7-8:
Torsion

Specimen 8

D = 508 mm
B = 305 mm
t = 7.15 mm
L = 5,553 mm
f'_c = 87.56 MPa
F_y = 365.4 MPa

Specimen 11

D = 508 mm; t = 5.98 mm;
L = 7,995 mm;
f'_c = 50.33 MPa; F_y = 328.0 MPa

Load Case 1

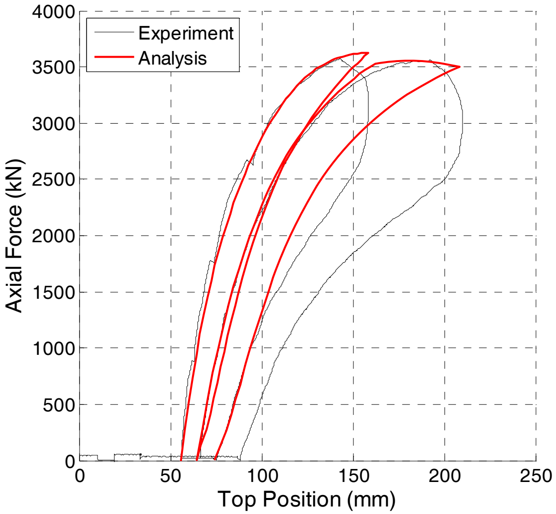

(a) Load Case 1: Concentric Loading

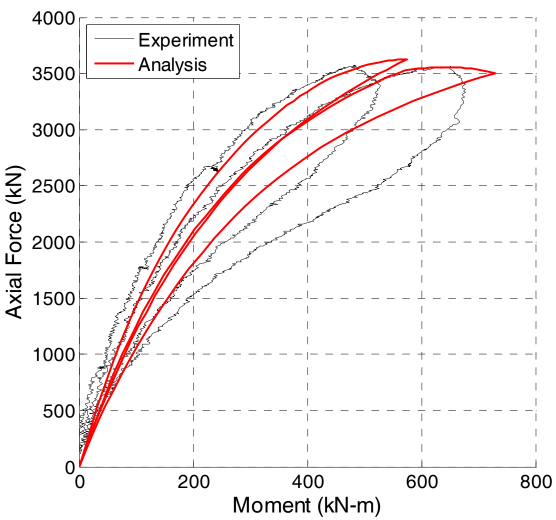

(b) Load Case 1: Concentric Loading

Load Case 2; P = 2,669 kN

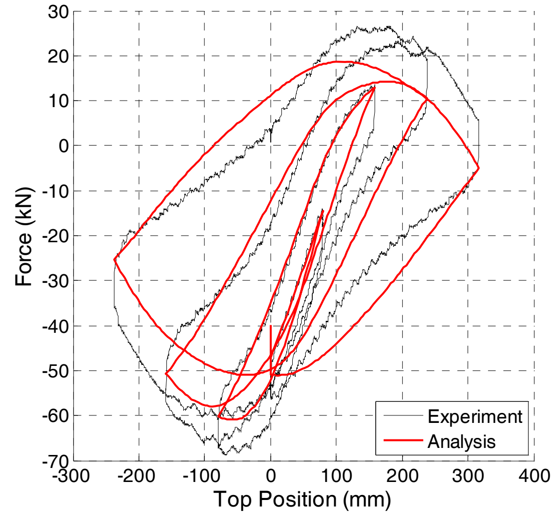

(c) Load Case 2: Uniaxial Cyclic

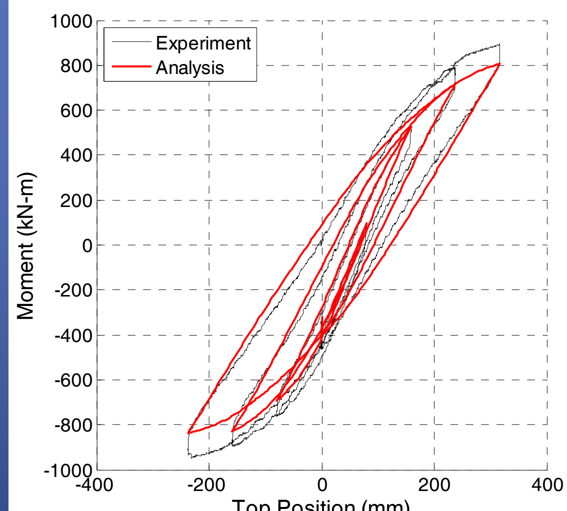

(d) Load Case 2: Uniaxial Cyclic

Load Case 3; P = 1,334 kN

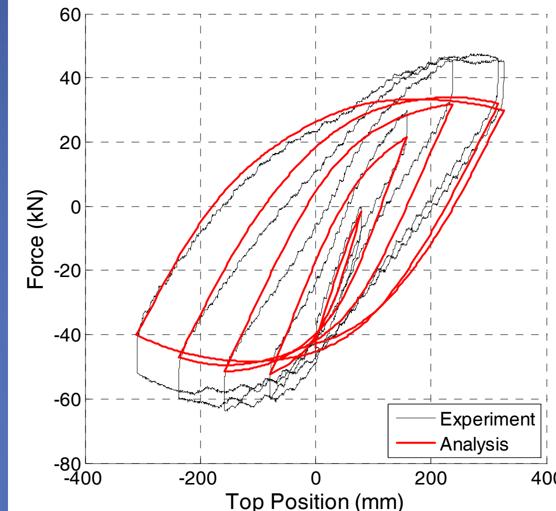

(e) Load Case 3: Uniaxial Cyclic

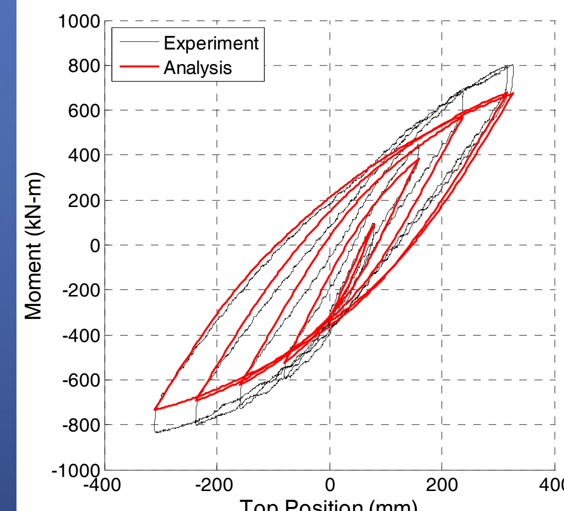

(f) Load Case 3: Uniaxial Cyclic

Specimen 11

D = 508 mm; t = 5.98 mm;
L = 7,995 mm;
f'_c = 50.33 MPa; F_y = 328.0 MPa

Load Case 4; P = 2,002 kN

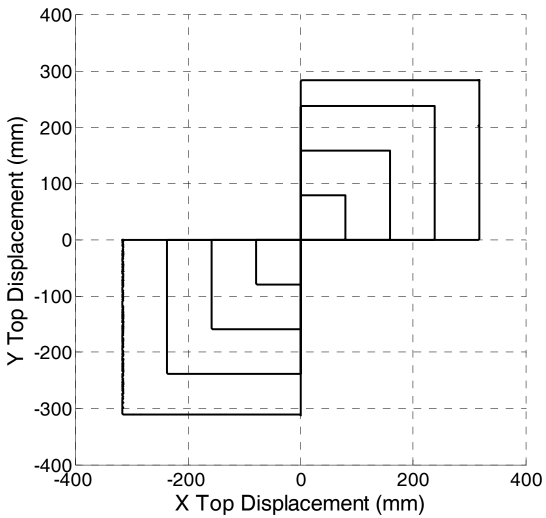

(g) Load Case 4: Biaxial Cyclic

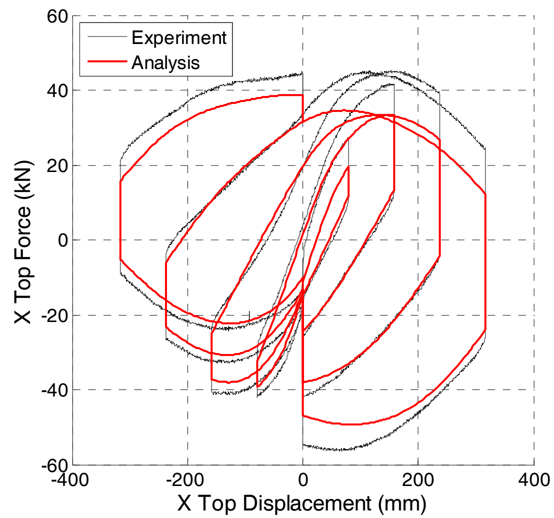

(i) Load Case 4: Biaxial Cyclic

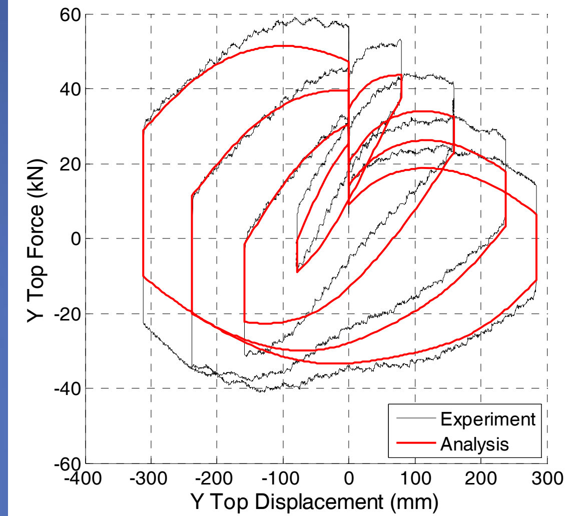

(i) Load Case 4: Biaxial Cvclic

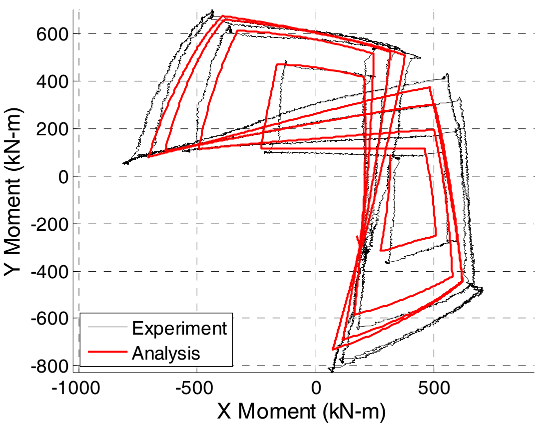

(h) Load Case 4: Biaxial Cyclic

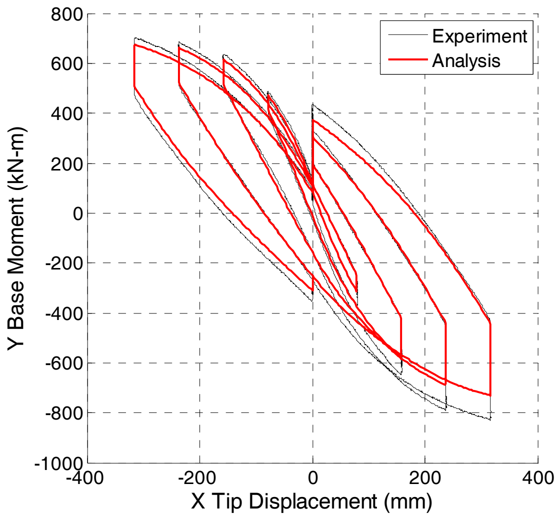

(k) Load Case 4: Biaxial Cyclic

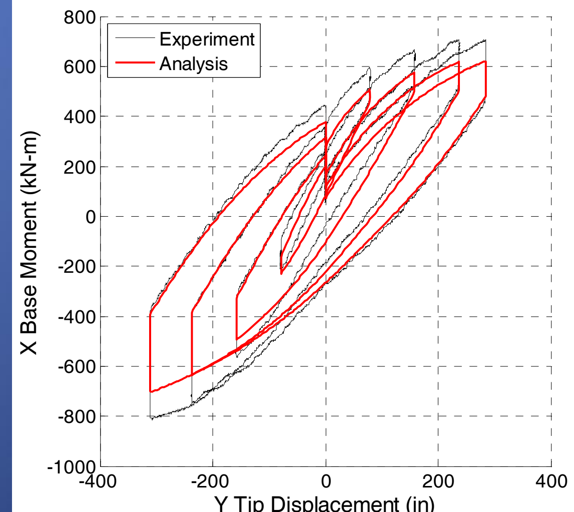

(l) Load Case 4: Biaxial Cyclic

Specimen 3

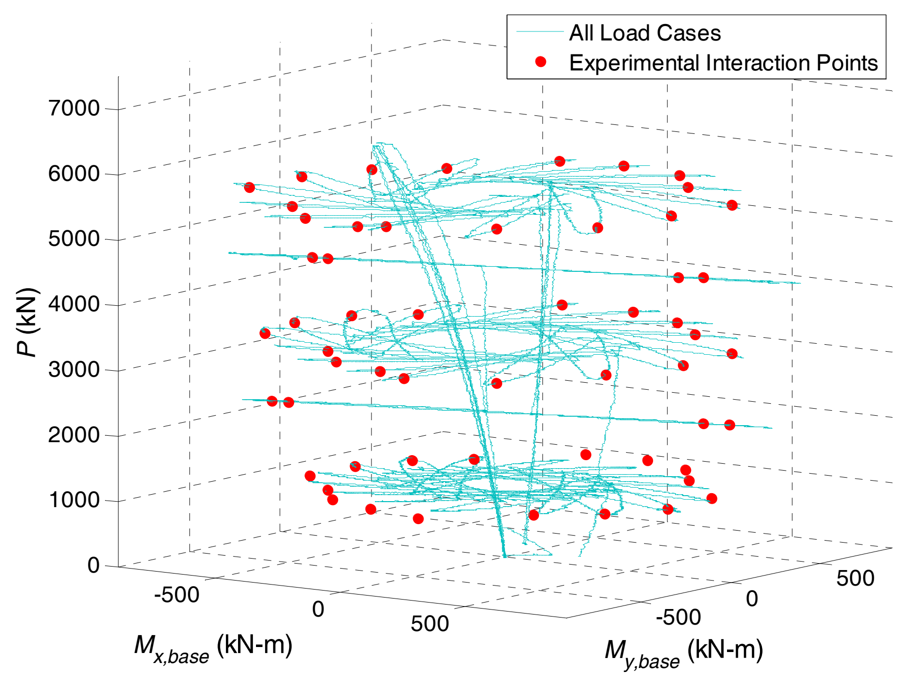

D = 508 mm; *t* = 5.98 mm;
L = 5,525 mm;
f'_c = 37.92 MPa; F_y = 328.0 MPa

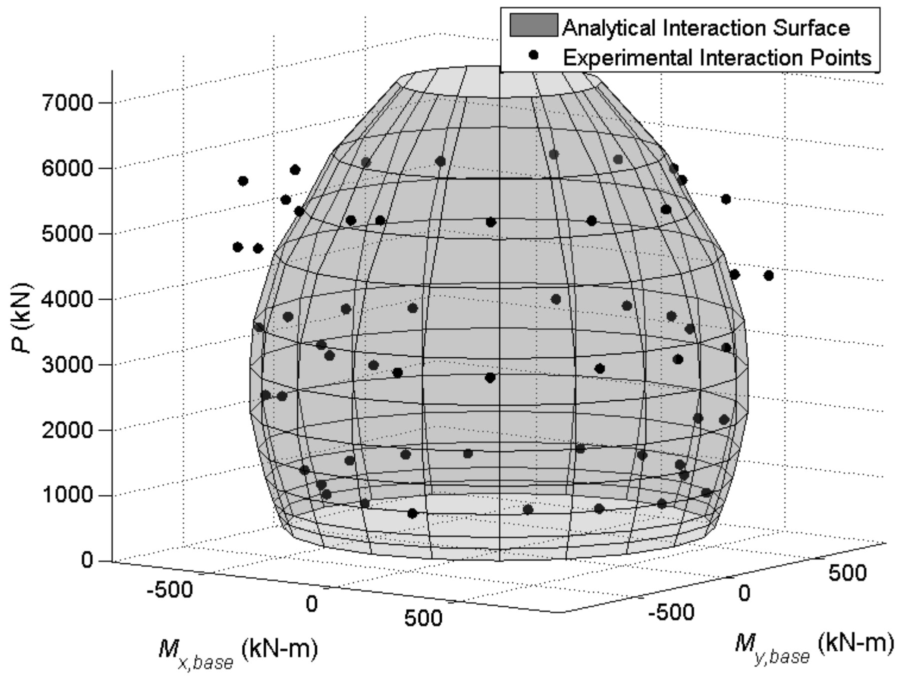

Concluding Remarks

- Experimental and computational research on CCFT and RCFT beam-columns
- An accurate nonlinear model has been developed for the analysis of circular concrete filled steel tubes
  - Accuracy confirmed by validation to a broad range of experimental results
  - Future research includes parametric studies
- Testing of the 18 beam-column specimens is complete
  - More detailed comparisons (e.g., at the section or material level) and conclusions are forthcoming based on more detailed data reduction